Catena 236 (2024) 107759

Contents lists available at ScienceDirect

Catena

journal homepage: www.elsevier.com/locate/catena

Identification and quantification of nutrients sources in the Aspio watershed (Italy). Insight from geogenic mineralization and anthropogenic pressure

Gianluigi Busico [a,b], Davide Fronzi [c], Nicolò Colombani [c,*], Micol Mastrocicco [a], Alberto Tazioli [c]

[a] Department of Environmental, Biological and Pharmaceutical Sciences and Technologies, Campania University "Luigi Vanvitelli", Via Vivaldi 43, 81100 Caserta, Italy
[b] Aristotle University of Thessaloniki, Department of Geology, Laboratory of Engineering Geology & Hydrogeology, 54124 Thessaloniki, Greece
[c] Department of Science and Engineering of Materials, Environmental Sciences and Urban Planning, Polytechnic University of Marche, Via Brecce Bianche 12, 60131 Ancona, Italy

ARTICLE INFO

Keywords:
SWAT
Urban runoff
Nutrients
Trend analysis
Land cover
Pollution sources

ABSTRACT

An accurate evaluation of river water quality could be challenging due to the complex hydrological and anthropogenic processes which affect its nature. Reliable water quality data are mandatory to identify long-term trends and regional variability at the watershed scale. In this study, a combined approach using time series, regression, and multivariate statistical analysis along with SWAT modelling was applied to identify the relevant hydrogeochemical processes and the nutrients sources within the Aspio watershed (Ancona, Italy). The analysis detected different processes: i) the geogenic origin of Cl^- and SO_4^{2-}, ii) the heavy metals (Cu and Ni) and hydrocarbons pollution due to runoff from urban and industrial areas, and iii) the agricultural contribution of pesticides, nitrogen, and phosphorous. A SWAT model was implemented to quantify the nutrients load in the Aspio river. A calibration for streamflow, river sediment yield, and for nutrients load was obtained considering agricultural, urban, and wastewater treatment plant contributions. Agriculture and treated wastewater contributed to the overall nitrogen load only for 4% and 12% respectively, while the majority was due to leakage from urban sewage (84%). A scenario with only fertilizers' load (excluding other sources) highlighted that nitrogen and phosphorous export from agricultural lands did not significatively impact the Aspio river. The spatial representation of runoff susceptibility also showed how the highest susceptibility for nitrogen and phosphorous loads is due to areas located close to urban settlements.

1. Introduction

The identification of point and diffuse pollution sources, along with the assessment of their possible impact upon environmental assets, such as soil and water ecosystem, is pivotal to ensure a sustainable exploitation of land and water resources on basin, regional, and national scales (Lam et al., 2010). Although the worldwide implementation of "Best Management Practices" (BMPs) aimed at reducing non-point pollution sources especially in farmed watersheds (e.g., buffer strips, fertilizer and manure reduction, grassland increase, and conservation tillage) (Geng et al., 2019), agricultural pollution is still the main environmental issue in several European countries (Malik et al., 2020; De Stefano et al., 2013). Indeed, pollutant transport from agricultural areas to surface water and groundwater bodies is one of the critical environmental issues currently faced by human societies (Reis et al., 2016).

Nitrogen (N) and phosphorus (P) are essential nutrients to ensure a sufficient crop yield, however, large-scale input of these nutrients to aquatic ecosystems was recognized as the primary cause of eutrophication and water quality depletion in both marine and freshwater systems (Hoagland et al., 2019).

Several factors are responsible for nutrients export, such as: i) irrigation and fertilizer management (McDowell, 2017; Nakamura et al., 2004), ii) soil characteristics (e.g., texture and organic carbon content) (Sogbedji et al., 2000), and iii) rainfall events pattern (Wang et al., 2014). In the last decades, many of these factors have been further exacerbated due to population growth, industrialization, growing demand of food production, climate variability and land use/management changes (Moss, 2012). Nitrate (NO_3^-) is recognized as the main

* Corresponding author.
E-mail address: n.colombani@univpm.it (N. Colombani).

https://doi.org/10.1016/j.catena.2023.107759
Received 8 February 2022; Received in revised form 5 October 2023; Accepted 13 December 2023
Available online 19 December 2023

anthropogenic pollutant worldwide (Ascott et al., 2017) and many policies have been developed to face this issue, like the European Water Framework Directive (E.U., 2000) and the Nitrates Directive (E.C., 1991), aiming to achieve a good ecological status for water bodies and to keep NO_3^- concentration below a threshold limit of 50 mg/L (E.U., 2000; E.C., 1991). An even more restrictive guideline was established by the World Health Organization (WHO) which fixed a NO_3^- concentration limit of 44 mg/L for drinking water (WHO, 2017; Briand et al., 2017). The same directives also regulate P concentration in surface waters.

The identification of pollution's sources along with a clear recognition of their contribution to the overall water quality status may provide technical support for an accurate formulation of basin management policies. Due to their temporal and spatial variations at the watershed scale, in response to hydrological and hydrochemical processes, such identification is particularly hard to achieve (Zhang and Huang, 2011). In fact, surface water quality can be simultaneously influenced by land use, river morphology, climate, and anthropogenic pollution (Lenart-Boron et al., 2017; Huang et al., 2014). Thus, continuous monitoring and analysis of surface water quality is a fruitful step to achieve a sustainable management of surface water resources (Ho et al., 2019; Kumar, 2019). Despite water quality monitoring and sampling are often costly and time-consuming, especially if performed continuously and over long periods, several monitoring networks have been implemented within the European basins and all over the world (Benfenati et al., 2003). Numerous studies focusing on time series and trend analysis were successfully developed in India (Lokhande and Tare, 2021), Malaysia (VishnuRadhan et al., 2017), China (Kumar, 2019), and Europe (Diamantini et al., 2018; Romero et al., 2016). These studies achieved the aim to identify and analyze the main water quality drivers along with their temporal and spatial variability. Other studies focused on forecasting surface water quality have been developed to identify possible future changes due to climate or landscape changes (Elhag et al., 2021; Bui et al., 2020; Dastorani et al., 2020). Similarly, multivariate statistical analysis (e.g., factor or principal component analysis) and trend analysis can produce accurate results in discriminating those hydrochemical processes responsible for groundwater quality and mineralization (Mastrocicco et al., 2021; Narany et al., 2018; Lloyd et al., 2014). Nevertheless, these methodologies cannot accurately quantify the contribution to the overall water quality status of each process acting in the watershed (Machiwal & Jha, 2012). For this purpose, process-based hydrological models could represent an effective tool to quantify the pollution loads coming from different sources within the same watershed (Liu et al., 2016). For instance, the Soil and Water Assessment Tool (SWAT) model is a process-based hydrological model widely used to simulate soil and nutrient losses derived by various management regimes (Zeiger et al., 2021; Noori et al., 2020; Lee et al., 2018; Serpa et al., 2017). Nevertheless, the use of process-based hydrological models is limited in those areas where detailed geospatial, climate, and monitoring data are not available (Wahren et al., 2016; Ntona et al., 2022). Recently, the applicability of process-based hydrological models has increased due to the availability of global and regional datasets containing geomorphological and climate information (Abbaspour et al., 2019; Shelestov et al., 2017).

Within this scenario, the aim of this research is to identify and quantify nutrients (N and P) load from point and diffuse pollution sources in the surface waters of the Aspio basin (Ancona, Italy). This basin was chosen because of peculiar hydrogeological and socio-economic characteristics: the presence of high density residential, industrial, and commercial settlements which contribute to reduce soil absorbing surfaces, right next to cultivated fields prone to fertilization with variable quantities of nutrients. The Aspio river water quality assessment from the Environmental Protection agency of the Marche Region (ARPAM, 2022) highlighted a persistently poor ecological status from 1999 to 2020. The major issues are due to elevated nutrients, Escherichia Coli, and COD, while pesticides and organic micropollutants are generally not elevated. Thus, the Aspio basin is affected by long-term contamination and still needs a clear conceptual model aimed at pollution sources identification and quantification. The current work can be divided into two main phases. First, regression, time series and multivariate statistical analysis were carried out on water quality parameters from 138 water samples collected bi-monthly from 1999 to 2019 at a single monitoring site located at the confluence of the basin. The primary objective was to identify the relationships between observed patterns of biophysical and chemical variables and the underlying natural or anthropogenic factors, including geologic interactions, agricultural practices, flow dynamics and population impacts. Then a multi-scenario process-based modelling with SWAT was implemented for the quantification of the main nutrient loads in the basin. A pre-existing SWAT model, applied in the same watershed for runoff susceptibility assessment (Busico et al., 2020a), was implemented with new data specifically collected and digitalized for the new elaboration regarding land use, land cover, agricultural management practices and information on the anthropogenic pollution sources.

2. Materials and methods

2.1. Study area

The Aspio watershed (Fig. 1), located south of Ancona in the Marche Region (Italy), spans over 155 km^2, with a minimum and maximum elevation of 8 m and 540 m above sea level. It is characterized by a smooth-surface hilly morphology and the Aspio river represents the main surface water course of the basin. The land use is heterogeneous (83 % agricultural, 2 % forest, 15 % urban), mainly dominated by urban settlements, that occupy the central part of the watershed, and agricultural fields located all around. The main crop is represented by wheat, followed by barley, corn, beet and sunflower. The basin is characterized by a Mediterranean climate with an average precipitation of 770 mm/y and a mean monthly temperature ranging between 3 °C in winter and 28 °C in summer, with an average annual temperature of 15 °C. The drainage basin of the Aspio river is characterized by a fast hydrological response due to the impermeable nature of the soils, to the high concentration of urban, commercial, and industrial activities along its terminal course, and to the existence of important communication routes, such as the A14 national highway and the national railway system (Busico et al., 2020a).

The geological setting of the Aspio watershed consists of different units: i) the Meso-Cenozoic limestone sequence, ii) the Mio-Plio-Pleistocene sequence made up of marly-clays, marly-clays with sandstone layers, and sandstone layers, and iii) the Quaternary continental deposits made up of silty clay, clayey sand, and eluvial-colluvial deposits (Tazioli et al., 2015). The main aquifer, hosted in the eluvial-colluvial deposits, feeds the Aspio river and its tributaries throughout the year and is responsible for the perennial surface water presence. Groundwater is characterized as Na-Cl type with high concentration of Mg^{2+} and SO_4^{2-}, especially close to the coastline where brackish waters seep from the Lower Pliocene geological formations (Comodi et al., 2011). The water supplies for drinking, industrial, and agricultural uses for most municipalities of the area are derived from local shallow aquifers.

2.2. Water quality datasets

For this study, selected physiochemical properties of the Aspio river at the closure of the basin (see Fig. 1 for location) provided by ARPAM (Agenzia Regionale per la Protezione Ambientale regione Marche) were used. A total of 138 samples were collected in wet and dry seasons from 1999 to 2019 to capture the water quality variability (see Supplementary Information). Among the large ARPAM database, which included a wide range of organic micropollutants and heavy metals, only selected parameters were retained: temperature (T), electrical conductivity (EC), pH, dissolved oxygen (O_2), total suspended solids (TSS), Escherichia Coli (ESR), chloride (Cl^-), bicarbonate (HCO_3^-), nitrate (NO_3^-), nitrite (NO_2^-),

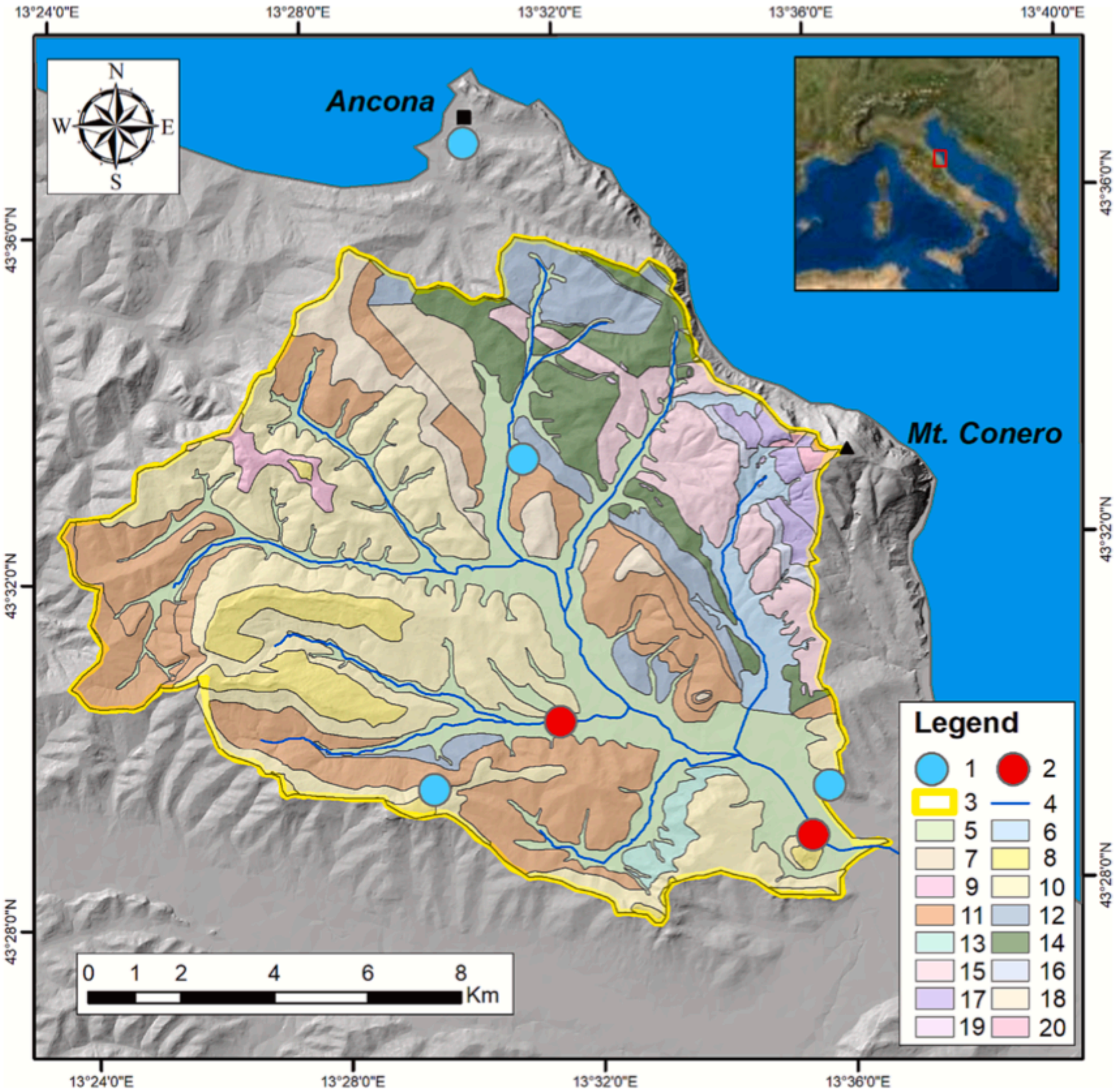

Fig. 1. Detailed lithological map of the study area. 1. Rainfall/temperature stations, 2. Hydrometric stations, 3. Aspio watershed, 4. Aspio river, 5. Alluvial-colluvial deposits, 6. Sandy terraced alluvial deposits, 7. Sandy-clays with gravel, 8. Stratified marly-clays, 9. Marly clays with sandstones, 10. Marly clays with sandy lenses, 11. Marly-clays, 12. Alternances of marly –clays and sands, 13. Marly limestones with sandstones, 14. Marls and Clay-marls, 15. Marly limestones, 16. Arenaceous limestones, 17. Stratified marly-limestones, 18. Sandy lenses with clays, 19. Gypsum, 20. Limestones.

ammonium (NH_4^+), sulphate (SO_4^{2-}), total hardness (Hard), biological oxygen demand (BOD), chemical oxygen demand (COD), total phosphorus (Ptot), phosphate (PO_4^{3-}), total pesticides (TP), and total hydrocarbons (TH). Temperature, EC, and pH were measured in situ, while samples intended for major ions, trace elements, and micropollutants analyses were collected in HDPE or glass bottles and analysed in a certified laboratory following the international standards guidelines (APHA, 2017).

2.3. Regression analysis

The first step of the work was the identification of all drivers responsible of river water quality through statistical analysis. The preprocessing consisted in a manual filtering of data to obtain a consistent period of overlapping between time series, excluding missing values pairwise. In fact, the sampling conducted by ARPAM does not include the analysis of all the chemical and physical parameters for the same sampling date (see Supplementary Information). Therefore, the original dataset was reduced to a 23x19 cells matrix containing 19 physiochemical parameters determined in 23 different sampling periods between May-1999 and March-2019. The matrix obtained has been used to explore any possible correlation between parameters, by maintaining the raw data provided by ARPAM with several data for each parameter > 20 as to have a statistically significant correlation. To assess the

correlation a "corrcoef" function in MATLAB® was selected. This is a simple and useful statistical method to calculate the Person's correlation coefficient between each pair of columns (A and B), following the equation (1):

$$\rho(A,B) = \frac{1}{n-1}\sum_{i=1}^{n}\left(\frac{A_i-\mu_A}{\sigma_A}\right)\left(\frac{B_i-\mu_B}{\sigma_B}\right) \quad (1)$$

where n is the amount of data for each element, μ_A and σ_A are the mean and standard deviation of A, and μ_B and σ_B are the mean and standard deviation of B. As a result, the correlation matrix between all the elements (R) is obtained as follows:

$$R = \begin{pmatrix} \rho(I_1,I_1) & \cdots & \rho(I_1,I_m) \\ \vdots & \ddots & \vdots \\ \rho(I_n,I_1) & \cdots & \rho(I_n,I_m) \end{pmatrix} \quad (2)$$

where I is the input matrix, n is the number of data and m is the number of elements.

For each computation, a p-value matrix to test the hypothesis of no correlation against the alternative hypothesis of a nonzero correlation was determined, with significance level of 0.05. After a rigorous evaluation, the sources of the elements within the analyzed basin have been hypothesized. The Spearman's rank correlation was applied to the water quality indicators and drivers to highlight those variables which could better represent the hydrogeochemical behavior of the basin.

2.4. Factor analysis

A multivariate statistical approach utilizing Factor Analysis (FA) has been employed to discern and characterize all the hydrogeochemical processes occurring in the Aspio basin. FA has emerged as a robust methodology, widely applied across various geoscience disciplines, enabling the elucidation of relationships among observed variables, and yielding a concise list of significant factors that encapsulate them. The determination of the number of factors is guided by the Kaiser criterion (Kaiser, 1960) and the overall validity of the analysis is assessed using the Kaiser-Meyer-Olkin (KMO) coefficient, which is deemed satisfactory when exceeding 0.5 (Kumar, 2014). Here 23 cases and 12 variables (BOD, COD, P_{Tot}, PO_4^{3-}, NO_3^-, NH_4^+, Cl^-, SO_4^{2-}, Ni, Cu, TH, and ESR) were used.

2.5. The soil and water assessment tool

The semi-distributed process-based hydrological model known as SWAT (Arnold et al., 1998; 2012), developed by the United States Department of Agriculture (USDA), is currently one of the most widely used watershed and river basin-scale model worldwide (Tan et al., 2020). SWAT can simulate and predict land management and climate change effects on hydrological components at basin scale. There are multiple major steps in developing a SWAT model that accurately simulates the land surface and transport processes of the watershed: i) the division of the watershed into multiple sub-watersheds according to its hydromorphologic characteristics, ii) the creation of the hydrologic response units (HRUs) which refer to all those portions characterized by a unique combination of land-use, slope, and soil attributes (Neitsch et al., 2000), and iii) the model's output calculation such as runoff, evapotranspiration (ET), aquifer recharge, sediment and nutrient loadings from each HRU and sub-basin. SWAT primary inputs include hydrometeorological data (using different timescale of input/output like daily precipitation, and daily, monthly, and yearly data for streamflow, or ET), soil and morphological characteristics, and the selection of biophysical processes (e.g., potential ET and channel routing). The information regarding plant initial growth (e.g., planting, initial leaf area index) and agricultural operations (e.g., application of fertilizers, pesticides, and tillage) can be specified in the model setup. The input data quality and resolution are responsible for output's reliability and uncertainty (Busico et al., 2020a). The output of runoff is calculated using two equations: i) a modified version of the curve number method (USDA, 2004), or ii) the Green–Ampt infiltration method. The Modified Universal Soil Loss Equation (MUSLE) (Williams, 1995) is used for sediment delivery calculation. The N cycle is simulated in the soil profile, considering five different organic and inorganic pools, with NO_3^- and NH_4^+ as inorganic forms. P is also simulated by SWAT in the soil by monitoring six different organic and inorganic pools. More details, explanation and description of all parameters involved in the SWAT setup can be found in Neitsch et al. (2010). Observed data of water quality and sediment/water flow are used to assess the reliability and the robustness of the methodology through a calibration and validation procedure. The free-standing software SWAT-CUP and specifically the Sequential Uncertainty Fitting version 2 (SUFI-2) algorithm (Abbaspour, 2015) is widely utilized for this purpose. SWAT-CUP investigates the most sensitive parameters that could influence the observed outputs within a fixed range of variation specifically designed by the operator (e.g.., ± 25 % of initial value). The results of the calibration and validation procedure, specifically the fitting between real and simulated data, are investigated using three well known statistical indices: i) coefficient of determination (R^2), ii) Nash-Sutcliffe efficiency (NSE), and iii) percent of bias (PBIAS), to be compared with the threshold proposed by Moriasi et al. (2007) (Table S1).

2.5.1. SWAT model setup

The SWAT model to quantify the river's sediment and nutrients (N and P) loads for the Aspio basin was realized using the ArcSWAT 2012 interface on ArcGIS 10.2, implementing a pre-existent calibrated SWAT model created for runoff susceptibility assessment (Busico et al., 2020a). New data about land use spatial discretization, land management operation, and pollution point sources has been added. The model delineates the watershed using a digital elevation model (DEM). Five classes of slope were created to account for morphology heterogeneity (<5, 5–10, 10–15, 15–20, >20). Soil characteristics were retrieved from the Digital Soil World Map (FAO, 2007) with a scale of 1:5 million, while land use/cover was classified according to the updated version of the Corine Land Cover (CLC, 2018), expressly produced for this study. Since the majority of watershed' soils have predominantly clayey characteristics, according to the results obtained by Busico et al., (2020a) and Chaplot (2005), it was not necessary to retrieve a more detailed soil distribution. Instead, a more in-depth definition of land use/cover classes for the Aspio basin was needed since the generic "agricultural fields" reported by CLC may include deciduous or evergreen commercial forests, grassland (herbaceous vegetation), or different crops (e.g., corn or wheat). These differences could greatly influence the SWAT modelling on streamflow, sediment, and especially on nutrients loads. The combination of slope, soil and land cover contribute to create the HRUs spatialization which were fixed to a maximum value of 500. The meteorological data on daily precipitation, maximum and minimum temperature were obtained from four stations (Osimo, Ancona, Baraccola, and Svarchi) of the Sistema Informativo Regionale Meteo-Idro-Pluviometrico (SIRMIP, 2020) located inside the Aspio basin (Fig. 1). Potential and actual ET were calculated using the Hargreaves module in SWAT since only precipitation and temperature data were used (Aschonitis et al., 2017). Daily streamflow data from two hydrometric stations (Scaricalasino and Outlet) recording from 2010 to 2019 were used for the calibration and validation procedure, along with daily scattered values of sediment transport, and nutrients concentrations (total N and P) recorded in the Outlet station.

2.5.2. Land cover/management refinement

The updated land cover map was produced using Google Earth images to refine the CLC (2018) classification. The CLC map is made of three progressively more detailed levels but not even the third level provides the information necessary for this study. For instance, the agricultural areas (level 1) in the study basin include the arable lands,

the heterogeneous agricultural areas, and permanent crops (level 2). The first two comprise "non-irrigated arable land" and "complex cultivation patterns (level 3). These classifications encompass several different crops (vegetables, corn, tobacco, aromatic, and more) which often require specific and incompatible managements. The latter are pivotal and diriment information to properly model N and P loads within a watershed and at its outlet, consequently, to fulfill the work's purpose a land use refinement was necessary. Starting from the CLC (2018) classification which identifies three main covers (agricultural, forestry, and urban areas), the land cover was updated using actual and historical images based on Landsat TM and ETM + satellites (Fig. 2). For this purpose, the use of Google Earth offers several advantages such as: i) the availability of satellite imagery with spatial resolution less than 1 m, ii) a full integration with GIS software, and iii) the possibility to visualize images of the same areas taken at different time (Malarvizhi et al., 2016). First, the CLC shapefile was intersected via spatial analyst tools with the sub-basins defined in the preliminary SWAT watershed analysis to obtain the main land cover for each sub-basin. Then, the Google Earth satellite images were imported in GIS environment as base maps of the previously produced shapefile. Finally, the shapefile was edited to reproduce the effective boundary of artificial, natural, and agricultural areas. The crop recognition was achieved using field images. Agricultural systems were divided into eight new covers identified as: corn, vineyards, orchards, sugar beet, sunflowers, barley, pasture, and wheat. Forests were divided into commercial (wood production) and natural ones, while urban areas were identified as commercial and residential ones. The management practices for each land cover are shown in Table S2. N and P requirements for the identified crops were obtained from "Linee guida nazionali di produzione integrata e relativi allegati" (Mipaaf, 2021) and from "Disciplinare di tecniche agronomiche di produzione integrata" (Regione Marche, 2011). These documents define the crops requirement of N and P aimed at minimizing the use of synthetic chemical compounds following the concept of rational fertilization (Table S3).

A point source of continuous input of N and P was identified in the wastewater treatment plant (WTP) of Camerano, located on the Aspio riverbank just before the Scaricalasino stream. In the WTP the raw sewage is subject to screening, sandblasting, and sedimentation treatments with separation of the activated sludge from the water phase, followed by disinfection and draining processes. The data of Camerano WTP were input in the SWAT model using the tool "point source" within the sub-basin N° 15 (Figure S1). The maximum N and P loads per day allowed by the Italian legislation for a WTP into surface water are 15 mg/l for N and 2 mg/l for P, which correspond to 97.5 kg-N/day and 13 kg-P/day considering a mean outflow of 6500 m^3/day. Other point sources (sub-basin N° 16, 21, and 33) of continuous input of N and P were identified in the septic tanks located in the urban settlements not connected with the WTP (Figure S1). The N and P loss from septic tanks in each settlement was estimated from the number of inhabitants, the average per capita daily water usage (215 l; https://www.istat.it), and the most reported concentration of N and P in raw septic tank effluent of 50 mg/l for N and 10 mg/l for P (Beal et al., 2005). The three urban settlements of Offagna (sub-basin 16), San Biagio (sub-basin 21), and Osimo (sub-basin 33) were considered since, according to municipality reports, in the years of simulation all wastewaters coming from these cities were not subjected to proper treatment and usually discharged in superficial courses. For Offagna, considering 1,984 habitants, the point source discharge was responsible for 218 kg-N/day and 4.31 kg-P/day, while San Biagio (1,651 habitants) was responsible for 181 kg-N/day and 3.32 kg-P/day. Finally, the city of Osimo, the biggest urban center of the three considered (34,918 habitants), was responsible for 3480 kg-N/day and 77 kg-P/day. Given the large uncertainty of the N and P concentrations due to the septic tanks, two additional scenarios were run with doubled and halved concentrations. These assumptions were imperative to attain a comprehensive understanding of the many processes affecting the surface water quality of the Aspio river, especially considering the absence of an ongoing monitoring infrastructure encompassing both WTP and municipal wastewater outflows. Consequently, the input source system was favored over the septic tank input within the SWAT module. This choice was dictated by the unavailability of data regarding the septic tanks location and geometric characteristics, as well as the corresponding N and P loads, all of which are vital for an accurate simulation. In comparison, the point source approach offered a more feasible and manageable implementation given the data limitations (Schilling and Wolter, 2009).

2.5.3. Model performance evaluation

The SWAT model was used to simulate streamflow, sediment, and nutrients loads for the period 2010–2018 using four years of warm-up (2010–2013). Two calibration runs were conducted: the initial run focused on streamflow utilizing monthly data, while the subsequent run utilized daily data for sediment, N, and P. Specifically, the second calibration incorporated the already calibrated streamflow parameters into a new project configured to produce daily output for the simulation. The parameters responsible for the streamflow simulation and utilized for the auto-calibration procedure were obtained from a previous SWAT

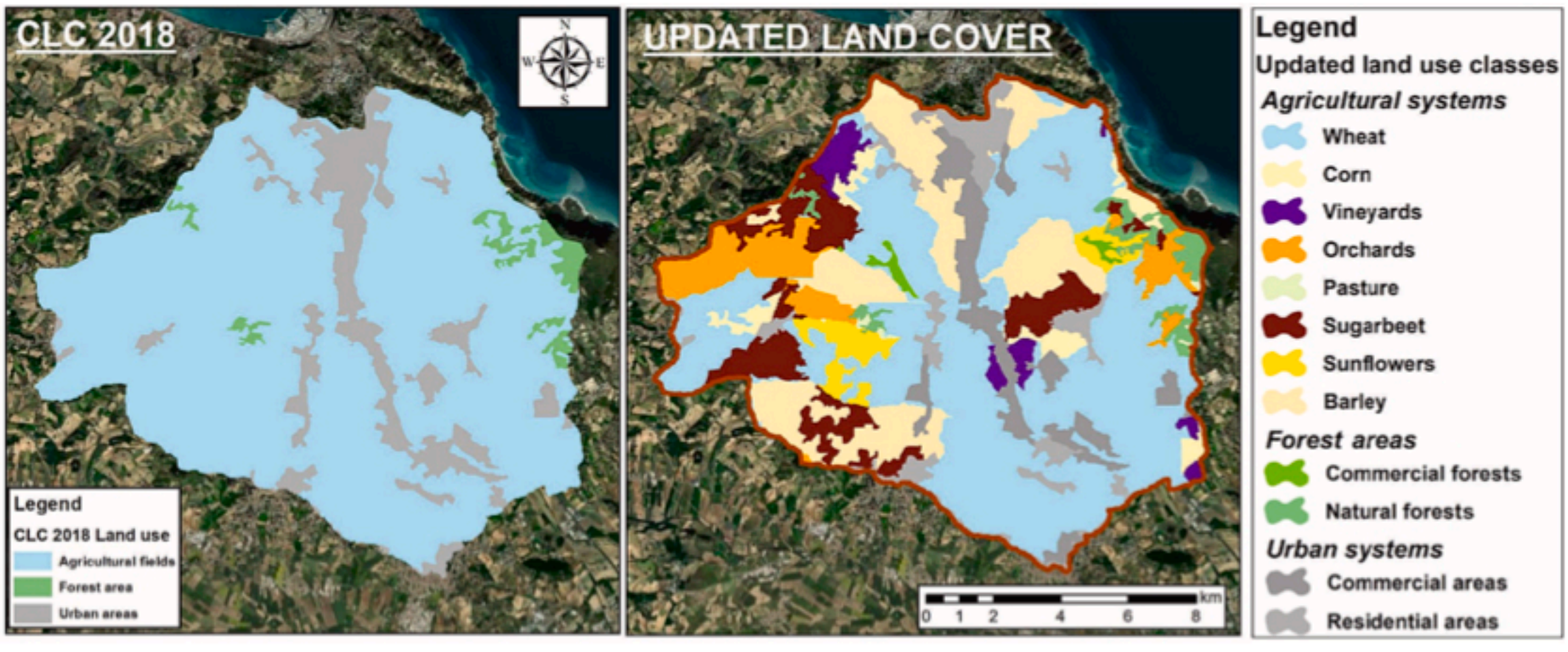

Fig. 2. Land use characterization of the Aspio watershed as identified from CLC (2018) (left panel) and according to the updated version (right panel).

application within the same watershed (Busico et al., 2020b), while those responsible of sediment and nutrients loads were identified through an extensive literature review (Table S4) (Malik et al., 2020; Chen et al., 2019; Khelifa et al., 2017). The SWAT-CUP program, and specifically the SUFI-2 algorithm, was utilized for the calibration and validation procedure. The available observed data (streamflow, sediment, N and P) from 01/01/2014 to 31/12/2016 were used to calibrate the model while the period from 01/01/2017 to 31/12/2018 was utilized for validation. For streamflow 84 monthly data were available while for sediment, N, and P only 17, 16 and 16 daily data were available, respectively. The NSE, PBIAS, and R^2 optimization functions were used to check the model reliability according to the performance values suggested by Moriasi et al. (2007) (Table S1). A total of three thousand calibration runs, divided in six interactions of five hundred runs each, were performed until a satisfactory calibration was obtained.

3. Results

3.1. Time series, correlation, and FA analysis

The step wise approach, used to implement a detailed model of the area, consisted in a preliminary statistical analysis among the elements in the pairwise time series (Table 1), which allowed to define and quantify the correlation between the parameters (Gibbons and Chakraborti, 2020) and to identify the best water quality indicators for the Aspio basin. The p-value matrix for testing the hypothesis of no correlation against the alternative hypothesis of a nonzero correlation is reported in the supplementary materials. The correlation matrix shows three strong correlations: i) Cl^- and SO_4^{2-}, ii) Ni, Cu, and NO_2^-, and iii) TH, ESR, and COD. The correlation among Cl^- and SO_4^{2-} (0.89) is ascribable to deep water upwelling characterized by high salinity (Comodi et al., 2011). This water, circulating in deep Pliocene deposits, can reach the surface through a deep system of faults which characterize the study area (Gobbi and Nanni, 1978). The correlation between Cu, Ni, and NO_2^- can be a sign of anthropogenic pollution from stormwater runoff in urban areas, which usually are sources of these metals and reactive N species (Czemiel Berndtsson, 2014; Pitt et al., 1999). The correlation between TH, ESR, and COD represents another anthropogenic process linked to the sewage leakage towards surface waters, from residential and industrial areas without proper treatment. The correlation among NH_4^+, NO_2^-, ESR, COD, and P_{tot} could further strengthen this hypothesis. FA identified 3 factors (F) with a KMO of 0.68 explaining more than 95 % of total variance (Table 2): F2 strengthens the correlation among Cl^- and SO_4^{2-} but showing only 12.5 % of variance; F1 which involves nutrients, heavy metals, and biological indicators, seems to be the main responsible of Aspio's water quality; F3 only involves ESR enforcing anthropogenic contribution already highlighted by F1.

To account and verify the agricultural contribution, all data on pesticides available in the dataset were merged into a unique parameter called TP. The time series comparison of TP versus TH (Fig. 2a) helps in stating the independence of the agricultural parameter TP from TH. In fact, the highest peak of TH corresponds to the lowest TP and vice versa. Moreover, to highlight the correlation or no-correlation between the elements, a data driven interpolating function between the elements was performed. Fig. 3b shows an example of correlation between TP and TH, where the hyperbolic function denoting the inverse relation between these parameters is supported by an acceptable correlation ($R = 0.623$ with p-value at 0.0005).

3.1.1. Sensitivity analysis

The result of the global sensitivity analysis indicating those parameters responsible for the simulated flow, nutrients, and soil losses are listed in Table S4. Specifically, 14 parameters were chosen as responsible of flow (DEEP_IMP, GW_DELAY, CN2, ESCO, RCHGR_DP), erosion (SLSUBBN, USLE_K, USLE_P, SPEXP, SPCON) and nutrient (NPERCO, PPERCO, CDN, ERORGP), according to the literature review (Busico

Table 1
Correlation matrix for the available parameters.

	T	ESR	O_2	pH	TSS	BOD	COD	P_{tot}	PO_4^{3-}	NO_3^-	NO_2^-	NH_4^+	Cl^-	SO_4^{2-}	EC	Hard	Ni	Cu	TH
T	1.00	−0.32	−0.40	0.00	0.26	0.20	0.05	0.20	0.15	−0.11	0.45	0.02	0.08	−0.09	−0.11	−0.09	0.49	0.48	−0.35
ESR	−0.32	1.00	−0.19	−0.26	0.09	−0.02	0.30	−0.03	−0.04	−0.19	0.03	0.18	−0.19	−0.11	0.13	0.19	0.07	−0.14	0.62
O_2	−0.40	−0.19	1.00	0.29	−0.39	0.19	−0.44	−0.16	−0.04	0.04	−0.15	−0.15	−0.04	0.02	0.32	0.11	−0.03	0.16	−0.05
pH	0.00	−0.26	0.29	1.00	0.03	0.14	−0.40	0.05	0.11	−0.09	0.01	−0.28	0.09	0.00	−0.04	−0.27	−0.07	0.10	−0.30
TSS	0.26	0.09	−0.39	0.03	1.00	−0.33	−0.27	0.36	−0.36	−0.33	−0.27	−0.23	−0.30	−0.18	−0.21	0.22	−0.01	−0.12	−0.14
BOD	0.20	−0.02	0.19	0.14	−0.33	1.00	0.06	0.30	0.22	−0.08	0.02	0.23	0.21	0.14	0.31	−0.12	0.33	0.58	−0.01
COD	0.05	0.30	−0.44	−0.40	−0.27	0.06	1.00	0.10	−0.04	−0.31	−0.49	0.66	0.21	0.02	−0.04	−0.19	0.54	0.13	−0.03
P_{tot}	0.20	−0.03	−0.16	0.05	−0.36	0.30	0.10	1.00	0.92	−0.12	0.44	1.00	0.18	0.05	0.19	−0.72	0.05	0.77	−0.41
PO_4^{3-}	0.15	−0.04	−0.04	0.11	−0.36	0.22	−0.04	0.92	1.00	−0.07	0.37	0.25	0.11	−0.02	0.00	−0.72	0.17	0.35	−0.19
NO_3^-	−0.11	0.45	−0.40	0.00	0.26	0.20	0.05	0.20	0.15	1.00	−0.49	−0.51	0.38	0.38	−0.08	0.02	−0.63	−0.37	−0.40
NO_2^-	0.45	−0.32	0.04	−0.15	0.27	−0.24	0.28	0.44	0.37	−0.49	1.00	0.66	0.21	0.11	0.27	0.37	−0.24	−0.41	0.01
NH_4^+	0.02	0.18	−0.15	−0.28	0.23	0.46	0.43	0.47	0.25	−0.51	0.66	1.00	0.18	0.17	0.33	−0.19	0.54	0.33	0.12
Cl^-	0.08	−0.19	1.00	0.09	−0.30	0.21	0.06	0.19	0.11	0.38	−0.49	0.18	1.00	0.89	0.34	−0.41	0.05	0.13	−0.13
SO_4^{2-}	−0.09	−0.11	0.02	0.00	−0.18	0.14	−0.04	0.02	0.00	0.38	−0.51	0.17	0.89	1.00	0.46	−0.20	−0.02	0.05	−0.03
EC	0.31	−0.12	0.14	−0.04	0.21	−0.31	0.02	−0.14	−0.11	0.06	−0.12	0.36	0.34	0.46	1.00	−0.20	−0.02	0.27	0.17
Hard	0.02	−0.19	0.09	0.00	0.22	−0.12	−0.19	−0.72	−0.72	0.02	−0.32	−0.24	−0.41	−0.20	−0.20	1.00	−0.19	−0.41	0.10
Ni	0.14	−0.72	0.22	0.11	−0.01	0.33	0.10	1.00	0.92	−0.63	0.86	0.54	0.05	−0.02	−0.02	−0.19	1.00	0.77	0.21
Cu	0.11	−0.72	0.35	0.01	−0.12	0.22	0.04	0.92	1.00	−0.37	0.85	0.33	0.13	0.05	0.17	−0.41	0.77	1.00	−0.03
TH	0.08	−0.40	0.05	−0.30	0.14	−0.40	0.58	0.10	−0.19	0.40	−0.37	−0.01	0.03	0.03	0.17	0.10	0.21	−0.03	1.00

ESR = Escherichia coli, TSS = Total suspended solid, BOD = Biological oxygen demand, COD = Chemical oxygen demand, Ptot = total Phosphorus, EC = Electrical conductivity, Hard = Total hardness, TH = Total hydrocarbon.

Table 2
Results of FA for the Aspio river.

	FACTORS		
	F1	F2	F3
Variance	74.2	12.5	9.66
BOD	**0.995**	0.023	0.011
COD	**0.980**	-0.077	0.008
P_{Tot}	**0.999**	-0.029	0.002
PO_4^{3-}	**0.999**	-0.028	0.000
NO_3^-	**0.945**	-0.058	-0.013
NH_4^+	**0.998**	-0.016	0.028
Cl^-	-0.050	**0.845**	-0.441
SO_4^{2-}	0.334	**0.850**	0.223
Ni	**0.997**	-0.005	-0.011
Cu	**0.996**	0.004	0.023
TH	**0.998**	-0.029	0.002
ESR	-0.157	0.194	**0.944**

et al., 2020a; Chen et al., 2019; Khelifa et al., 2017; Serpa et al., 2015). The significance of the sensitivity test was evaluated using the statistical index "p-value", automatically generated through the application of the SUFI-2 algorithm. The results of the sensitivity analysis for each simulated process highlighted that: i) the streamflow simulation is strongly dependent from the distance to the impervious layer (DEEP_IMP), the groundwater delay time (GW_DELAY), and the SCS curve number (CN2), ii) the USLE parameters (USLE_K and USCLE_P) and the slope length (SLSUBBSN) are the main parameters influencing sediment losses, and iii) the P and N percolation factors (P_PERCO, N_PERCO) are responsible for the nutrients loadings.

3.1.2. Streamflow and sediment simulation

SWAT demonstrated to successfully simulate both streamflow and sediment regimes in the Aspio watershed (Fig. 4a, 4b). For the streamflow calibration, the results showed a "very good" agreement between simulated and measured data, with satisfactory values of R^2, NSE, and PBIAS in both hydrometric stations.

Similarly, the statistical indices for validation were within the range of a "very good" model performance. Moreover, analyzing the two hydrometric regimes of Scaricalasino (Fig. 4a) and Outlet stations (Fig. 4b), the model proved to adequately simulate both low and high regime of streamflow. Considering the sediment load calibration, where randomly distributed daily sediment data (2014–2018) were used, the simulation was again classified as "very good" (Fig. 4c).

3.1.3. Nutrients loading simulation

The calibration results for N and P loads at the watershed closure (Outlet station) are shown in Fig. 5. Despite the "very good" simulation obtained for discharge and erosion, N and P simulations were considered "good" given the relatively low number of observed concentrations. The results of statistical indices are shown in Table 3. The "good" evaluation can be justified accordingly with the results proposed by Moriasi et al. (2007) (Table S1). Specifically, in case of daily scattered data for nutrients' simulation, the evaluation of R^2 and PBIAS is enough to judge the simulation efficiency. Fig. 5 shows the comparison among simulated and observed values of N and P for the Outlet station. Despite showing big differences in absolute values, the trends highlighted by the grey area, which summarize the minimum and maximum N and P concentrations in septic tanks, are fully comparable ($R^2 > 0.7$) with the observed concentrations. To show the impact of the WPT and the septic tanks on the overall nutrients export in the Aspio river, a scenario with only agricultural inputs was run. The results depicted in Fig. 5 (dashed line) highlight that fertilizer leaching in the simulated period is minimal (two order of magnitude lower) with respect to the other sources.

3.1.4. Erosion and nutrients export

Susceptibility maps of for sediment, N, and P exports throughout superficial runoff were generated using the HRUs output and only considering the agricultural diffuse source of pollution, without involving punctual anthropogenic source of pollution (Fig. 6). Similarly, to Busico et al., (2020a), the susceptibility maps were created averaging the results for the whole simulation period and then classified in five classes of susceptibility from "very low" to "very high" using the geometrical interval. The yearly N amount leached in superficial runoff range from 0 to 41 kg-N/ha/year, P range from 0 to 0.71 kg-P/ha/year, while sediment yield ranges from 0 to 11 t/ha/year. In the Aspio basin only the susceptibility classes from medium to very high are represented. The sediment load perfectly matches with the steeper morphology and agricultural areas (wheat, corn, and sunflower), while N and P exports mainly correspond to corn cultivations and to the urban areas where leaching from septic tanks is particularly conspicuous and represent the major component of nutrient release at the basin scale. Anyway, the maximum yearly amounts of nutrient leached from the surrounding area does not justify the N and P value monitored in the Aspio river.

4. Discussion

According to the Global Environment Monitoring System database (Robarts et al., 2002), NO_3^- concentration in several rivers around the world could reach values three to seven times higher than the healthy water quality standard of 10 mg/L suggested by WHO (He et al., 2011). In the Aspio river, according to the monitoring system of ARPAM, the value of NO_3^- and NH_4^+ reached a maximum concentration of 55 mg/L and 11 mg/L respectively, with an average value of 18 mg/l for NO_3^- and 2.25 for NH_4^+ During the period of analysis (2004–2019) NO_3^- exceeded the suggested threshold limit of 10 mg/L in river water 70 % of time. Hence, an accurate investigation focusing on nutrients sources identification and quantification is mandatory. The time series, regression,

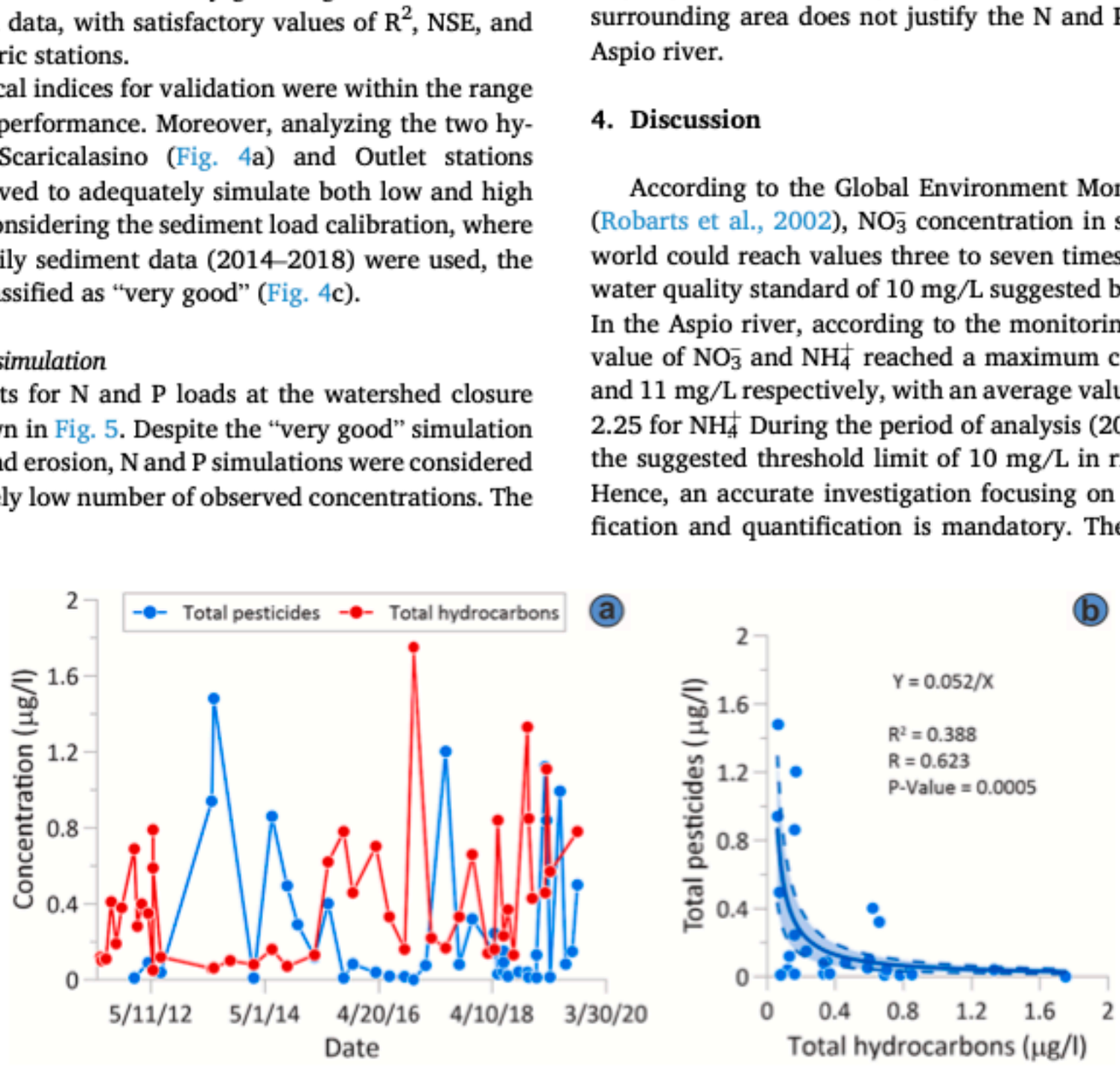

Fig. 3. Comparison among Total pesticides and Total hydrocarbons time series (a), and their hyperbolic relation (b).

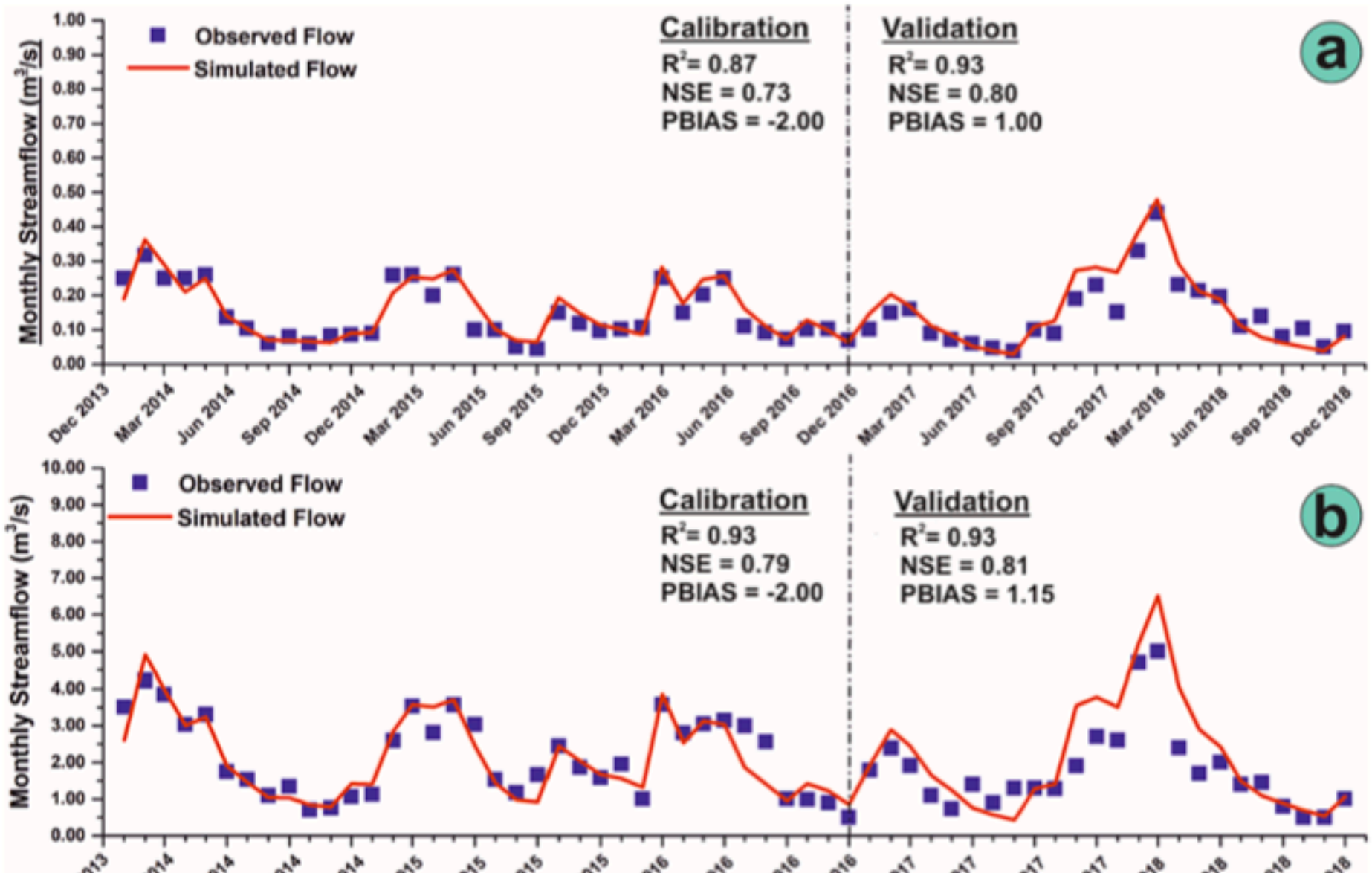

Fig. 4. Calibration and validation for the streamflow simulation in the two hydrometric stations of Scaricalasino (a) and Outlet (b); calibration and validation for the sediment load simulation (c).

and multivariate statistical analysis, allowed to identify the main hydrochemical processes and to correctly quantify the role of the geogenic mineralization while the process-based hydrological models was useful to identify and quantify pollution sources. Specifically the first allowed to obtain an accurate hydrochemical characterization of the Aspio river waters, identifying four main processes: i) geogenic, related to the upwelling of deep saline water rich in SO_4^{2-} and Cl^- which are prevailing during drought periods when the baseflow component is dominant, ii) heavy metal pollution (Cu and Ni) due to the rainwater runoff from industrial and urban areas, iii) a probable wastewater contamination (TH, ESR, NH_4^+, and COD), and iv) agricultural contribution (TP). N species along with P, due to their correlation with biological indicator and heavy metals might derive from several sources such as: fertilizers, septic tanks, WTP, and urban runoff (Busico et al., 2017; Li et al., 2011). The SWAT model was applied to quantify the different sources (agricultural, WTP, and septic tanks) contribution to river nutrients input. The methodology proved to adequately simulate both streamflow and sediment loads and provided satisfactory results also for N and P loads. Specifically, the simulation considering' only agricultural input of N and P, was impossible to calibrate since other pollution sources beyond the agricultural contribution were present. Since in the SWAT routine the main sources of N and P are soil organic matter, fertilizers, WTP, and septic tanks inputs (Abbaspour et al., 2015), the latter represents the only pollution sources which are probably responsible for the large nutrients loading rate in the Aspio river. So, to calculate the overall contribution in percentage of each source, an average value (within calibration and validation points) of real nutrient concentrations has been calculated and then compared with the various SWAT output. According to this calculation, the pollutant sources in the Aspio watershed could be ranked as follow (Table 3): i) N agricultural load is equivalent to 4 ± 1 % of the whole N load of the Aspio river, ii) WTP contribution is responsible for 12 ± 1 % of the N load, considering a stable discharge and a nutrient outflow never upon the legal limits, and iii) the remaining 84 ± 5 % can be ascribable to leakage from septic tanks, occurring especially in rural settlements not connected to WTPs (Górski et al., 2019; Lu et al., 2008; Wakida and Lerner, 2005). For P instead, the agricultural load due to fertilizers runoff accounts for only 4 ± 1 %, while WTP and other anthropogenic activities could be equally responsible for the remaining load.

Moreover, significant P losses could be ascribable to the soil eroded

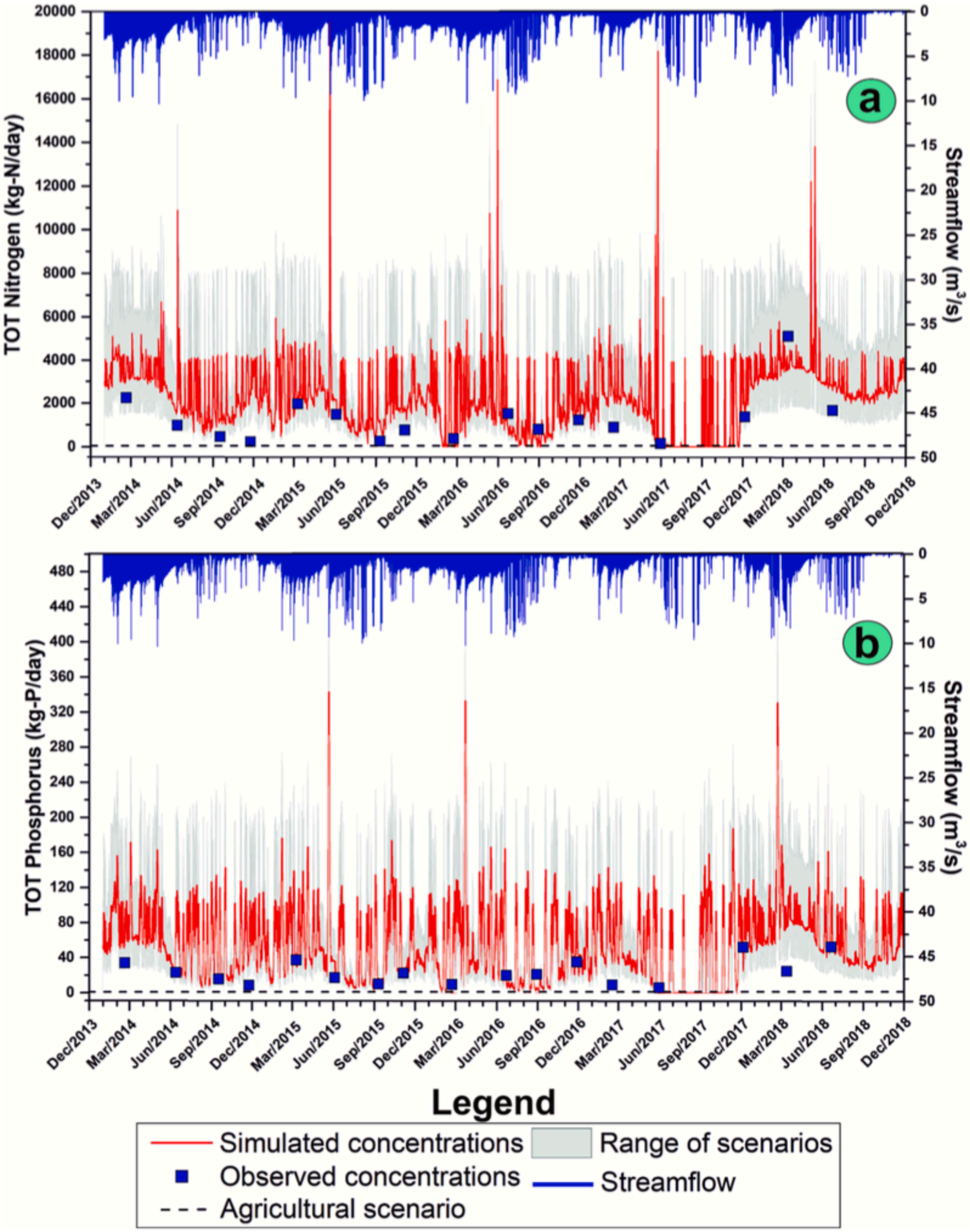

Fig. 5. Calibration diagrams for Nitrogen (a) and Phosphorous (b) loads at the Outlet station.

from agricultural land (Schoumans et al., 2014), especially in those areas with high susceptibility (Fig. 6) which could represent an important pathway of P migration. Anyway, is important to highlight that such application could retrieve better and more reliable results if at least monthly data of nutrient loads would be available. The uncertainties due to the inherent impossibility to precisely characterize N and P loading rates from the septic tanks are highlighted in Fig. 5, where the range of the doubled and halved N and P concentrations have been used. Despite the daily concentrations are extremely variable, their mass uncertainties are relatively limited as highlighted in Table 4. Indeed, this study

Table 3
Summary of statistical indices for SWAT simulation.

	Calibration			Validation		
	R^2	NSE	PBIAS	R^2	NSE	PBIAS
Streamflow	0.93	0.79	−2.00	0.93	0.81	−1.00
Sediment	0.86	0.82	2.40	0.91	0.85	1.06
Nitrogen	0.65	0.48	−12.00	0.71	0.51	−6.50
Phosphorous	0.68	0.45	0.10	0.73	0.42	1.30

emphasized the utility of time series, regression, and multivariate analysis as valuable tools for discerning the various processes responsible for water quality. It also sheds light on the limitations of these methods when it comes to accurately quantifying the magnitude of each process, particularly in situations where the same pollutant is associated with multiple phenomena.

The Water Framework Directive demanded the accomplishment of good ecological status of rivers throughout the EU by 2015, but this was seldom achieved except for a few cases (Boets et al., 2021; Romero et al., 2016). Moreover, it required to invert rising trends in organic and inorganic contaminants concentrations. In the Aspio watershed, no significant improvement has been recorded after 2015, with very high concentrations of ESR still present in 2019 (Supplementary Material), as well as anionic surfactants which are a clear indication of septic tanks losses. As highlighted in this study, advanced resolution of different nutrients sources and their spatial distribution is required to precisely evaluate the risk of eutrophication in anthropized watersheds. This aim can be attained by integrating a preliminary pollution sources analysis along with watershed solute transport modeling. The combined application of these two methods proves particularly advisable in basins characterized by uncertainties pertaining to pollution sources, especially in cases where a comprehensive monitoring system is lacking. From a decision-making point of view, water quality managers of the Aspio watershed could focus on increasing the number of houses and buildings connected to WTPs or promote better maintenance of septic tanks in rural settlements located near the streams, while the agricultural nutrients load seems to be a minor concern.

Table 4
Discrimination of N and P sources in the Aspio watershed: septic tanks, fertilizers and WTP.

Pollution sources	NITROGEN	PHOSPHORUS
Septic tanks	84 ± 5 %	48 ± 3 %
Fertilizers	4 ± 1 %	4 ± 1 %
WTP	12 ± 1 %	48 ± 2 %

The uncertainty is calculated from the scenarios with different N and P concentrations in septic tanks.

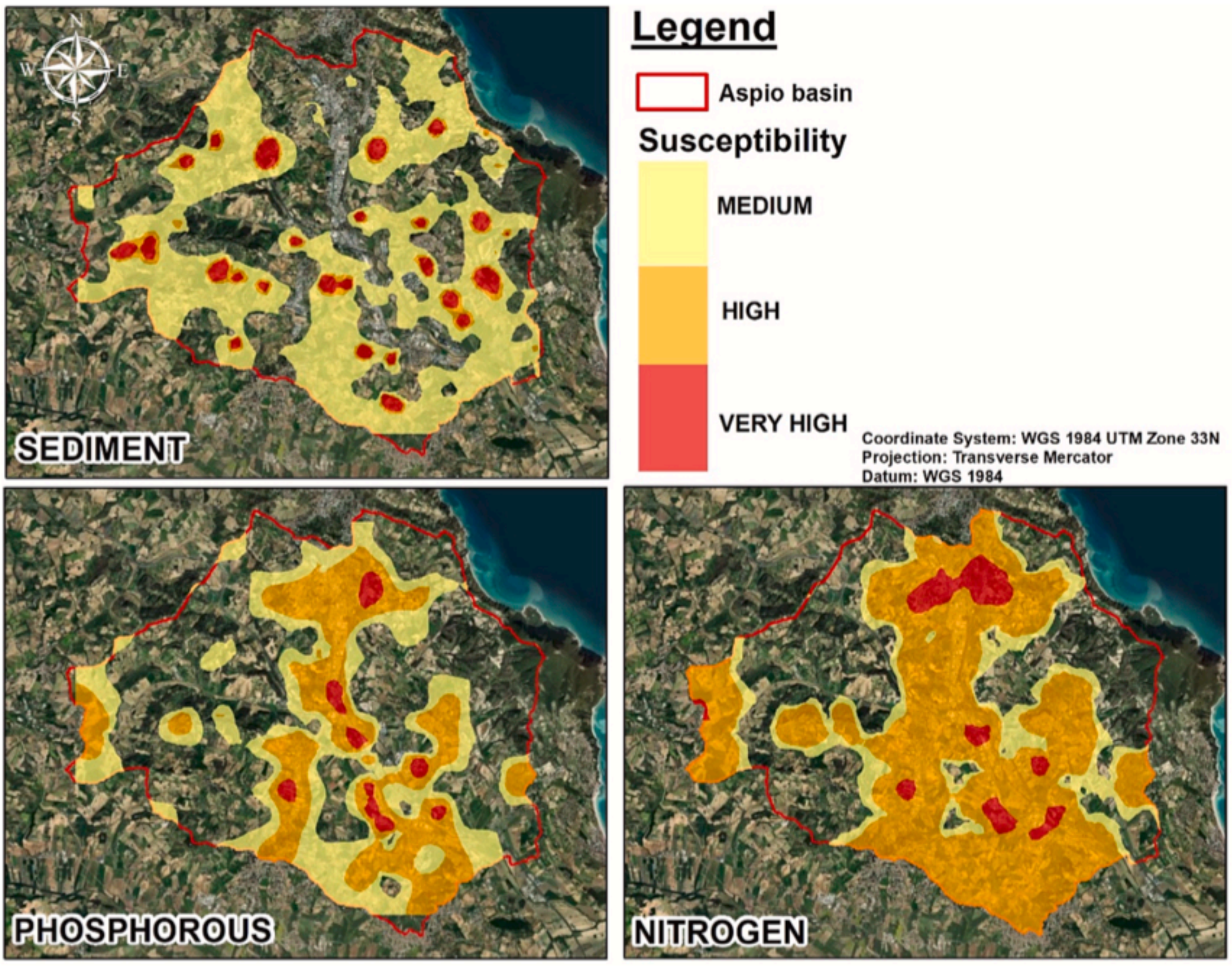

Fig. 6. Susceptibility map for sediment, N, and P exports.

5. Conclusions

SWAT model application supported by a detailed time series analysis and regression analysis on a robust database allowed to identify and quantify the nutrient loads in the Aspio watershed. NO_3^- showed no significant correlation with other parameters indicating multiple sources. The agricultural contribution plays a minor role representing only 4 ± 1 % of the whole river load, despite the occurrence of agricultural activities in most of the watershed. On the other hand, few areas occupied by civil, commercial, and industrial settlements have a much greater impact on river's pollution, mainly due to septic tanks' effluents. Also for P, agricultural contribution is minimal and other activities/processes, like WTP and septic tanks, represent the main sources contributing to P load in the Aspio river. The proposed approach to discriminate nutrients sources in the Aspio basin could be easily replicated in similar watersheds where the origin of nutrients loads is unknown, or the information is fragmentary. The availability of such studies could promote sound management and policy strategies designed to protect and/or improve the quality of surface waters, with targeted measures that primarily focus on the recognition and mitigation of the most significant nutrient sources at the watershed scale.

Declaration of Competing Interest

The authors declare that they have no known competing financial interests or personal relationships that could have appeared to influence the work reported in this paper.

Data availability

Data will be made available on request.

Acknowledgements

The authors thank Dr. Debora Mancaniello of the Marche Agency for Environmental Protection for the kind and profitable collaboration and for providing the Aspio water quality data.

Appendix A. Supplementary data

Supplementary data to this article can be found online at https://doi.org/10.1016/j.catena.2023.107759.

References

Abbaspour, K.C., 2015. Calibration and uncertainty programs. SWAT-cup User Manual.
Abbaspour, K.C., Rouholahnejad, E., Vaghefi, S., Srinivasan, R., Yang, H., Kløve, B., 2015. A continental-scale hydrology and water quality model for Europe: calibration and uncertainty of a high-resolution large-scale SWAT model. J. Hydrol. 524, 733–752. https://doi.org/10.1016/j.jhydrol.2015.03.027.
Abbaspour, K.C., Vaghefi, S.A., Yang, H., Srinivasan, R., 2019. Global soil, land-use, evapotranspiration, historical and future weather databases for SWAT applications. Sci. Data. 6, 263. https://doi.org/10.1038/s41597-019-0282-4.
American Public Health Association (APHA) (2017). Standard Methods for the Examination of Water and Wastewater. 23rd edition. American Public Health Association, American Water Works Association, and Water Environment Federation, Washington DC, 1268 pp. ISBN: 978-0-87553-287-5.
Arnold, J.G., Srinivasan, R., Muttiah, R.S., Williams, J.R., 1998. Large-area hydrologic modeling and assessment: Part I. Model development. J. Am. Water Resour. Assoc. 34, 73–89. https://doi.org/10.1111/j.1752-1688.1998.tb05961.x.
Arnold, J.G., Moriasi, D.N., Gassman, P.W., Abbaspour, K.C., White, M.J., Srinivasan, R., Santhi, C.R., Harmel, D., van Griensven, A., Van Liew, M.W., Kannan, N., Jha, M.K., 2012. SWAT: model use, calibration, and validation. Trans. ASABE 55 (4), 1491–1508. https://doi.org/10.13031/2013.42256.
ARPAM, 2022. Technical Reports on surface water quality (in Italian). Available online at https://www.arpa.marche.it/comunicazione/pubblicazioni-arpa-marche Last access on 03/06/2022.
Aschonitis, V.G., Papamichail, D., Demertzi, K., Colombani, N., Mastrocicco, M., Ghirardini, A., Castaldelli, G., Fano, E.A., 2017. High-resolution global grids of revised Priestley-Taylor and Hargreaves-Samani coefficients for assessing ASCE standardized reference crop evapotranspiration and solar radiation. Earth Syst. Sci. Data 9, 615–638. https://doi.org/10.5194/essd-9-615-2017.
Ascott, M.J., Gooddy, D.C., Wang, L., Stuart, M.E., Lewis, M.A., Ward, R.S., Binley, A.M., 2017. Global patterns of nitrate storage in the vadose zone. Nat. Commun. 8, 1416. https://doi.org/10.1038/s41467-017-01321-w.
Beal, C.D., Gardner, E.A., Menzies, N.W., 2005. Process, performance, and pollution potential: a review of septic tank-soil absorption systems. Austral. J. Soil Res. 43, 781–802. https://doi.org/10.1071/SR05018.
Benfenati, E., Barcelò, D., Johnson, I., Galassi, S., Levsen, K., 2003. Emerging organic contaminants in leachates from industrial waste landfills and industrial effluent. TrAC Trends Anal. Chem. 22 (10), 757–765. https://doi.org/10.1016/S0165-9936(03)01004-5.
Boets, P., Dillen, A., Mertens, J., Vervaeke, B., Van Thuyne, G., Breine, J., Goethals, P., Poelman, E., 2021. Do investments in water quality and habitat restoration programs pay off? An analysis of the chemical and biological water quality of a lowland stream in the Zwalm River basin (Belgium). Environ. Sci. Pol. 124, 115–124. https://doi.org/10.1016/j.envsci.2021.06.017.
Briand, C., Sebilo, M., Louvat, P., Chesnot, T., Vaury, V., Schneider, M., Plagnes, V., 2017. Legacy of contaminant N sources to the NO3- signature in rivers: a combined isotopic (δ15N-NO3−, δ18O-NO3−, δ11B) and microbiological investigation. Sci. Rep. 7 (1), 41703. https://doi.org/10.1038/srep41703.
Bui, D.T., Khosravi, K., Tiefenbacher, J., Nguyen, H., Kazakis, N., 2020. Improving prediction of water quality indices using novel hybrid machine-learning algorithms. Sci. Tot. Enviro. 721, 137612 https://doi.org/10.1016/j.scitotenv.2020.137612.
Busico, G., Colombani, N., Fronzi, D., Pellegrini, M., Tazioli, A., Mastrocicco, M., 2020a. Evaluating SWAT model performance, considering different soils data input, to quantify actual and future runoff susceptibility in a highly urbanized basin. J. Environ. Manag. 266, 110625 https://doi.org/10.1016/j.jenvman.2020.110625.
Busico, G., Kazakis, N., Cuoco, E., Colombani, N., Tedesco, D., Voudouris, K., Mastrocicco, M., 2020b. A novel hybrid method of specific vulnerability to anthropogenic pollution using multivariate statistical and regression analyses. Water Res. 171, 115386 https://doi.org/10.1016/j.watres.2019.115386.
Chaplot, V., 2005. Impact of DEM mesh size and soil map scale on SWAT runoff, sediment, and NO3-N loads predictions. J. Hydrol. 312 (1–4), 207–222. https://doi.org/10.1016/j.jhydrol.2005.02.017.
Chen, Y., Xu, C.-Y., Chen, X., Xu, Y., Yin, Y., Gao, L., Liu, M., 2019. Uncertainty in simulation of land-use change impacts on catchment runoff with multi-timescales based on the comparison of the HSPF and SWAT models. J. Hydrol. 573, 486–500. https://doi.org/10.1016/j.jhydrol.2019.03.091.
Corine Land Cover - CLC (2018).
Comodi, G., Cioccolanti, L., Palpacelli, S., Tazioli, A., Nanni, T., 2011. Distributed generation and water production: a study for a region in central Italy. Desalin. Water Treat. 31 (1–3), 218–225. https://doi.org/10.5004/dwt.2011.2375.
Czemiel Berndtsson, J., 2014. Storm water quality of first flush urban runoff in relation to different traffic characteristics. Urban Water J. 11 (4), 284–296. https://doi.org/10.1080/1573062X.2013.795236.
Dastorani, M., Mirzavand, M., Dastorani, M.T., Khosravi, H., 2020. Simulation and prediction of surface water quality using stochastic models. Sustain. Water Resour. Manag. 6, 74. https://doi.org/10.1007/s40899-020-00430-7.
De Stefano, L., Martínez-Santos, P., Villarroya, F., Chico, D., Martínez-Cortina, L., 2013. Easier said than done? The establishment of baseline groundwater conditions for the implementation of the Water Framework Directive in Spain. Water Resour. Manag. 27, 2691–2707. https://doi.org/10.1007/s11269-013-0311-6.
Diamantini, E., Lutz, S.R., Mallucci, S., Majone, B., Merz, R., Bellin, A., 2018. Driver detection of water quality trends in three large European river basins. Sci. Tot. Environ. 612, 49–62. https://doi.org/10.1016/j.scitotenv.2017.08.172.
Elhag, M., Gitas, I., Othman, A., Bahrawi, J., Psilovikos, A., Al-Amri, N., 2021. Time series analysis of remotely sensed water quality parameters in arid environments, Saudi Arabia. Environ. Dev. Sustain. 23 (2), 1392–1410. https://doi.org/10.1007/s10668-020-00626-z.
European Council - E.C. (1991). Council of the European Communities CEC, 1991. Council Directive 91/676/EEC concerning the protection of waters against pollution caused by nitrates from agricultural sources. Off. J. L 375.
Geng, R., Yin, P., Sharpley, A.N., 2019. A coupled model system to optimize the best management practices for nonpoint source pollution control. J. Clean. Prod. 220, 581–592. https://doi.org/10.1016/j.jclepro.2019.02.127.
Gibbons, J.D., Chakraborti, S. (2020). Nonparametric statistical inference. Chapman and Hall CRC press, 694 pp. ISBN 9781138087446.
Gobbi, G., Nanni, T., 1978. Caratteristiche idrochimiche delle acque del subalveo del F. Aspio (Ancona). Stud. Geol. Cam. 4, 75–87. https://doi.org/10.15165/studgeocam-1334.
Górski, J., Dragon, K., Kaczmarek, P.M.J., 2019. Nitrate pollution in the Warta River (Poland) between 1958 and 2016: trends and causes. Environ. Sci. Pollut. Res. 26, 2038–2046. https://doi.org/10.1007/s11356-017-9798-3.
He, B., Kanae, S., Oki, T., Hirabayashi, Y., Yamashiki, Y., Takara, K., 2011. Assessment of global nitrogen pollution in rivers using an integrated biogeochemical modeling framework. Water Res. 45 (8), 2573–2586. https://doi.org/10.1016/j.watres.2011.02.011.
Ho, J.Y., Afan, H.A., El-Shafie, A.H., Koting, S.B., Mohd, N.S., Jaafar, W.Z.B., Hin, L.S., Malek, M.A., Ahmed, A.N., Mohtar, W.H.M., Elshorgaby, A., El-Shafie, A., 2019. Towards a time and cost-effective approach to water quality index class prediction. J. Hydrol. 575, 148–165. https://doi.org/10.1016/j.jhydrol.2019.05.016.
Hoagland, B., Schmidt, C., Russo, T.A., Adams, R., Kaye, J., 2019. Controls on nitrogen transformation rates on restored floodplains along the Cosumnes River California. Sci. Tot. Environ. 649, 979–994. https://doi.org/10.1016/j.scitotenv.2018.08.379.
Huang, J., Huang, Y., Zhang, Z., 2014. Coupled effects of natural and anthropogenic controls on seasonal and spatial variations of river water quality during baseflow in a

coastal watershed of southeast China. PLoS One 9 (3), 91528. https://doi.org/10.1371/journal.pone.0091528.
Kaiser, H.F., 1960. The application of electronic computers to factor analysis. Educ. Psychol. Meas. 20, 141–151.
Khelifa, W.B., Hermassi, T., Strohmeier, S., Zucca, C., Ziadat, F., Boufaroua, M., Habaieb, H., 2017. Parameterization of the effect of bench terraces on runoff and sediment yield by swat modeling in a small semi-arid watershed in northern Tunisia. Land Degrad. Dev. 28 (5), 1568–1578. https://doi.org/10.1002/ldr.2685.
Kumar, P., 2014. Evolution of groundwater chemistry in and around Vaniyambadi industrial area: differentiating the natural and anthropogenic sources of contamination. Chem. Erde 74, 641–651. https://doi.org/10.1016/j.chemer.2014.02.002.
Kumar, P., 2019. Numerical quantification of current status quo and future prediction of water quality in eight Asian megacities: challenges and opportunities for sustainable water management. Environ. Monit. Assess. 191, 319. https://doi.org/10.1007/s10661-019-7497-x.
Lam, Q.D., Schmalz, B., Fohrer, N., 2010. Modelling point and diffuse source pollution of nitrate in a rural lowland catchment using the SWAT model. Agric. Water. Manag. 97 (2), 317–325. https://doi.org/10.1016/j.agwat.2009.10.004.
Lee, S., Sadeghi, A.M., McCarty, G.W., Baffaut, C., Lohani, S., Duriancik, L.F., Thompson, A., Yeo, I.Y., Wallace, C., 2018. Assessing the suitability of the soil vulnerability index (SVI) on identifying croplands vulnerable to nitrogen loss using the SWAT model. Catena 167, 1–12. https://doi.org/10.1016/j.catena.2018.04.021.
Lenart-Boron, A., Wolanin, A., Jelonkiewicz, E., Zelazny, M., 2017. The effect of anthropogenic pressure shown by microbiological and chemical water quality indicators on the main rivers of Podhale, southern Poland. Environ. Sci. Pollut. Res. 24 (14), 12938–12948. https://doi.org/10.1007/s11356-017-8826-7.
Li, J., Li, H., Shen, B., Li, Y., 2011. Effect of non-point source pollution on water quality of the Weihe river. Int. J. Sediment Res. 26 (1), 50–61. https://doi.org/10.1016/S1001-6279(11)60075-9.
Liu, R., Xu, F., Zhang, P., Yu, W., Men, C., 2016. Identifying non-point source critical source areas based on multi-factors at a basin scale with SWAT. J. Hydrol. 533, 379–388. https://doi.org/10.1016/j.jhydrol.2015.12.024.
Lloyd, C.E., Freer, J.E., Collins, A.L., Johnes, P.J., Jones, J.I., 2014. Methods for detecting change in hydrochemical time series in response to targeted pollutant mitigation in river catchments. J. Hydrol. 514, 297–312. https://doi.org/10.1016/j.jhydrol.2014.04.036.
Lokhande, S., Tare, V., 2021. Spatio-temporal trends in the flow and water quality: response of river Yamuna to urbanization. Environ. Monit. Assess. 193, 117. https://doi.org/10.1007/s10661-021-08873-x.
Lu, Y., Tang, C., Chen, J., Sakura, Y., 2008. Impact of septic tank systems on local groundwater quality and water supply in the Pearl River Delta, China: case study. Hydrol. Proces. 22 (3), 443–450. https://doi.org/10.1002/hyp.6617.
Machiwal, D., Jha, M.K. (2012). Current Status of Time Series Analysis in Hydrological Sciences. In: Hydrologic Time Series Analysis: Theory and Practice. Springer, Dordrecht. DOI: 10.1007/978-94-007-1861-6_6.
Malarvizhi, K., Vasantha Kumar, S., Porchelvan, P., 2016. Use of high-resolution google earth satellite imagery in landuse map preparation for urban related applications. Procedia Technol. 24, 1835–1842. https://doi.org/10.1016/j.protcy.2016.05.231.
Malik, W., Jiménez-Aguirre, M.-T., Dechmi, F., 2020. Coupled DSSAT-SWAT models to reduce off-site N pollution in Mediterranean irrigated watershed. Sci. Tot. Environ. 745, 141000 https://doi.org/10.1016/j.scitotenv.2020.141000.
Regione Marche (2011). Disciplinare di tecniche agronomiche di produzione integrata. Legge 03/02/2011, n. 4.
Mastrocicco, M., Gervasio, M.P., Busico, G., Colombani, N., 2021. Natural and anthropogenic factors driving groundwater resources salinization for agriculture use in the Campania plains (Southern Italy). Sci. Tot. Environ. 758 https://doi.org/10.1016/j.scitotenv.2020.144033.
McDowell, R.W., 2017. Does variable rate irrigation decrease nutrient leaching losses from grazed dairy farming? Soil Use Manag. 33 (4), 530–537. https://doi.org/10.1111/sum.12363.
Ministero delle Politiche Agricole Alimentari e Forestali - Mipaaf (2021). https://www.reterurale.it/flex/cm/pages/ServeBLOB.php/L/IT/IDPagina/22126.
Moriasi, D., Arnold, J., Van Liew, M., Bingner, R., Harmel, R., Veith, T., 2007. Model evaluation guidelines for systematic quantification of accuracy in watershed simulations. Trans. ASABE 50 (3), 885–900. https://doi.org/10.13031/2013.23153.
Moss, B., 2012. Cogs in the endless machine: Lakes, climate change and nutrient cycles: a review. Sci. Tot. Environ. 434, 130–142. https://doi.org/10.1016/j.scitotenv.2011.07.069.
Nakamura, K., Harter, T., Hirono, Y., Horino, H., Mitsuno, T., 2004. Assessment of root zone nitrogen leaching as affected by irrigation and nutrient management practices. Vadose Zone J. 3 (4), 1353–1366. https://doi.org/10.2113/3.4.1353.
Narany, T.S., Sefie, A., Aris, A.Z., 2018. The long-term impacts of anthropogenic and natural processes on groundwater deterioration in a multilayered aquifer. Sci. Tot. Environ. 630, 931–942. https://doi.org/10.1016/j.scitotenv.2018.02.190.
Neitsch, S., Arnold, J., Kiniry, J., Srinivasan, R., Williams, J., 2010. Soil and Water Assessment Tool: Input/OutputFile Documentation, Version 2009. USDA-ARS, Grassland, Soil and Water Research Laboratory, Temple, Tex.
Neitsch, S., Arnold, J., Kiniry, J., Williams, J. (2000). Soil and Water Assessment Tool Theoretical Documentation 2000. Grassland, Soil and Water Research Laboratory, Agricultural Research Service, 808 East Blackland Road, Temple, Texas 76502:506.
Noori, N., Kalin, L., Isik, S., 2020. Water quality prediction using SWAT-ANN coupled approach. J. Hydrol. 590, 125220 https://doi.org/10.1016/j.jhydrol.2020.125220.
Ntona, M.M., Busico, G., Mastrocicco, M., Kazakis, N., 2022. Modeling groundwater and surface water interaction: an overview of current status and future challenges. Sci. Total Environ. 846, 157355 https://doi.org/10.1016/j.scitotenv.2022.157355.
Pitt, R., Clark, S., Field, R., 1999. Groundwater contamination potential from stormwater infiltration practices. Urban Water 1 (3), 217–236. https://doi.org/10.1016/S1462-0758(99)00014-X.
Reis, S., Bekunda, M., Howard, C.M., Karanja, N., Winiwarte, W., Yan, X., Bleeker, A., Sutton, M.A., 2016. Synthesis and review: tackling the nitrogen management challenge: from global to local scales. Environ. Res. Lett. 11, 120–205. https://doi.org/10.1088/1748-9326/11/12/120205.
Robarts, R.D., Fraser, A.S., Hodgson, K.M., Paquette, G.M., 2002. Monitoring and assessing global water quality-the GEMS-Water experience. Int. J. Ecohydrol. Hydrobiol. 1 (2), 19–27.
Romero, E., Le Gendre, R., Garnier, J., Billen, G., Fisson, C., Silvestre, M., Riou, P., 2016. Long-term water quality in the lower seine: lessons learned over 4 decades of monitoring. Environ. Sci. Pol. 58, 141–154. https://doi.org/10.1016/j.envsci.2016.01.016.
Schilling, K.E., Wolter, C.F., 2009. Modeling nitrate-nitrogen load reduction strategies for the des moines river. Iowa Using SWAT Environ. Manag. 44 (4), 671–682. https://doi.org/10.1007/s00267-009-9364-y.
Schoumans, O.F., Chardon, W.J., Bechmann, M.E., Gascuel-Odoux, C., Hofman, G., Kronvang, B., Rubaek, G.H., Ulen, B., Dorioz, J.-M., 2014. Mitigation options to reduce phosphorus losses from the agricultural sector and improve surface water quality: a review. Sci. Tot. Environ. 468–469, 1255–1266. https://doi.org/10.1016/j.scitotenv.2013.08.061.
Serpa, D., Nùnes, J.P., Santos, J., Sampaio, E., Jacinto, R., Veiga, S., Lima, J.C., Moreira, M., Corte-Real, J., Keizer, J.J., Abrantes, N., 2015. Impacts of climate and land use changes on the hydrological and erosion processes of two contrasting Mediterranean catchments. Sci. Tot. Environ. 538, 64–77. https://doi.org/10.1016/j.scitotenv.2015.08.033.
Serpa, D., Nunes, J.P., Keizer, J.J., Abrantes, N., 2017. Impacts of climate and land use changes on the water quality of a small Mediterranean catchment with intensive viticulture. Environ. Pollut. 224, 454–465. https://doi.org/10.1016/j.envpol.2017.02.026.
Shelestov, A., Lavreniuk, M., Kussul, N., Novikov, A., Skakun, S., 2017. Exploring google earth engine platform for big data processing: Classification of multi-temporal satellite imagery for crop mapping. Front. Earth Sci. 5, 1–10. https://doi.org/10.3389/feart.2017.00017.
Sistema Informativo Regionale Meteo-Idro-Pluviometrico – SIRMIP (2020). http://app.protezionecivile.marche.it/sol/indexjs.sol?lang=it.
Sogbedji, J.M., Es, H.M., Yang, C.L., Geohring, L.D., Magdoff, F.R., 2000. Nitrate leaching and nitrogen budget as affected by maize nitrogen rate and soil type. J. Environ. Qual. 29, 1813–1820. https://doi.org/10.2134/jeq2000.00472425002900060011x.
Tan, M.L., Gassman, P.W., Yang, X., Haywood, J., 2020. A review of SWAT applications, performance and future needs for simulation of hydro-climatic extremes. Adv. Water Resour. 143 https://doi.org/10.1016/j.advwatres.2020.103662.
Tazioli, A., Mattioli, A., Nanni, T., Vivalda, P.M. (2015). Natural hazard analysis in the Aspio equipped basin. In: Engineering geology for society and territory, Volume 3: River basins, reservoir sedimentation and water resources, 431-435. DOI: 10.1007/978-3-319-09054-2_89.
European Union - E.U. (2000). Directive 2000/60/EC of the European Parliament and of the Council of 23 October 2000 establishing a framework for community action in the field of water policy. Official Journal of the European Union L 327-72, 22/12/2000.
United States Department of Agriculture - USDA (2004). National Engineering Handbook, Part 630 – Hydrology, Chapter 9: Hydrologic Soil-Cover Complexes.
VishnuRadhan, R., Zainudin, Z., Sreekanth, G.B., Dhiman, R., Salleh, M.N., Vethamony, P., 2017. Temporal water quality response in an urban river: a case study in peninsular Malaysia. Appl. Water. Sci. 7, 923–933. https://doi.org/10.1007/s13201-015-0303-1.
Wahren, F.T., Julich, S., Nunes, J.P., Gonzalez-Pelayo, O., Hawtree, D., Feger, K.-H., Keizer, J.J., 2016. Combining digital soil mapping and hydrological modeling in a data scarce watershed in north-central Portugal. Geoderma 264, 350–362. https://doi.org/10.1016/j.geoderma.2015.08.023.
Wakida, F.T., Lerner, D.N., 2005. Non-agricultural sources of groundwater nitrate: a review and case study. Water Res. 39 (1), 3–16. https://doi.org/10.1016/j.watres.2004.07.026.
Wang, Z., Li, J., Li, Y., 2014. Simulation of nitrate leaching under varying drip system uniformities and precipitation patterns during the growing season of maize in the north China plain. Agric. Water Manag. 142, 19–28. https://doi.org/10.1016/j.agwat.2014.04.013.
Williams, J.R., 1995. Chapter 25: The EPIC Model. In: Singh, V.P. (Ed.), Computer Models of Watershed Hydrology. Water Resources Publications, Highlands Ranch, U.S., pp. 909–1000
World Health Organization - WHO, 2017. Guidelines for Drinking-Water Quality, fourth ed. World Health Organization.
Zeiger, S.J., Owen, M.R., Pavlowsky, R.T., 2021. Simulating nonpoint source pollutant loading in a karst basin: a SWAT modeling application. Sci. Tot. Environ. 785, 147295 https://doi.org/10.1016/j.scitotenv.2021.147295.
Zhang, H., Huang, G.H., 2011. Assessment of non-point source pollution using a spatial multicriteria analysis approach. Ecol. Model. 222 (2), 313–321. https://doi.org/10.1016/j.ecolmodel.2009.12.011.